Conformation Rearrangement and Molecular Dynamics of Poly(3-hydroxybutyrate) during the Melt-Crystallization Process Investigated by Infrared and Two-Dimensional Infrared Correlation Spectroscopy

Jianming Zhang,[†] Harumi Sato,[†] Isao Noda,[‡] and Yukihiro Ozaki*,[†]

Department of Chemistry, School of Science and Technology, Kwansei-Gakuin University, Gakuen, Sanda 669-1337, Japan, and The Procter & Gamble Company, 8611 Beckett Road, West Chester, Ohio 45069

Received January 21, 2005; Revised Manuscript Received March 4, 2005

ABSTRACT: Time-dependent infrared (IR) spectral variations during isothermal melt-crystallization process of poly(3-hydroxybutyrate) (PHB) have been analyzed for different wavenumber regions (C−H, C═O, C−O−C, and C−C stretching vibration regions) by difference spectra, second derivatives, and two-dimensional (2D) correlation analysis, and the bands characteristic of crystalline and amorphous parts are identified in each region. By the 2D correlation analysis, it has been found that the intensity changes in the 1731 cm^{-1} band, which may be due to the intermediate state, and in the 1722 cm^{-1} band due to the crystal packing occur out of phase with each other, whereas those in the two amorphous C═O stretching bands (1747 and 1739 cm^{-1}) ascribed to the different conformations of the main chain are synchronous, which represents a cooperative conformational rearrangement for the C═O groups in the amorphous state during the crystallization process. Meanwhile, a distinct delay between the intensity change rates of bands at 1184 and 825 cm^{-1} indicates that the adjustment of C−O−C backbone occurs faster than that of C−C backbone in PHB. This result has also been confirmed by investigating the 2D correlation spectra of PHB in various spectral regions. On the basis of these observations, a physical picture on the molecular evolution of PHB during the melt-crystallization process has been derived.

1. Introduction

The crystallization process of polymer that transfers the entangled melt into a semicrystalline state is one of the most important research topics in polymer physics and has been studied for a long time.[1] Thermodynamically, polymer crystallization is a first-order transition that involves overcoming an energy barrier. Building a molecular kinetic model that links this macroscopic concept with experimental observations has been and still remains a difficult issue.[2−6] It requires a physical picture that can show how a three-dimensionally random linear macromolecule is converted to a chain-folded crystalline state despite the loss of entropy in the process. Lotz and Cheng et al.[4,5] suggested that, in polymer crystallization, every macromolecule has to go through several selection processes on different length and time scales. Moreover, on the basis of broad and detailed evidence from a large variety of experiments on several polymer systems carried out by other research groups and themselves, Strobl[6] proposed a novel crystallization model which indicates that the formation and growth of lamellar crystallites are a multistep process passing over intermediate states, although the exact definition on the intermediate states is not provided. The understanding of the crystallization process of polymer based on the knowledge of the molecular mobility controlling the transformation is still lacking.

It is well documented that Fourier transform infrared spectroscopy (FTIR) is sensitive to the conformation and local molecular environment of polymers.[7,8] More specifically, the structural formation of chain segment conformations, helical chain conformations, and chain packing during the crystallization can be followed by monitoring different characteristic bands. Although one cannot "see" a single molecular trajectory during the polymer crystallization process, macromolecular dynamics in the crystallization processes can be in principle probed at the different molecular levels or length scales by real-time IR spectroscopy. Thus, FTIR has been extensively used as a powerful tool for investigating the crystallization process of semicrystalline polymers.[9−12] However, because of some limitation of the conventional spectral analysis methods, certain useful information on the crystallization dynamics could not have been easily "decoded" from the overlapped IR spectral changes. Generalized two-dimensional (2D) correlation spectroscopy, introduced by Noda in 1993,[13−15] has become a powerful and versatile tool for elucidating subtle spectral changes induced by an external perturbation.

In a generalized 2D correlation spectroscopy experiment, a series of perturbation-induced dynamic spectra are collected first in a systematic manner, e.g., in a sequential order during a temperature-, concentration-, or time-dependent process. Such a set of dynamic spectra is then transformed into a set of 2D correlation spectra by a cross-correlation analysis. Some of the most notable features of 2D correlation spectra are simplification of complex spectra consisting of many overlapped peaks, enhancement of spectral resolution by spreading peaks along the second dimension, establishment of unambiguous assignments through the correlation of bands selectively coupled by various interaction mechanism, and identified the specific order of certain events taking place under the influence of a controlled physical variable. These features are ideally suited for the study

[†] Kwansei-Gakuin University.
[‡] The Procter & Gamble Company.
* To whom all correspondence should be addressed: Fax +81-79-565-9077; e-mail ozaki@ksc.kwansei.ac.jp.

10.1021/ma0501343 CCC: $30.25
Published on Web 04/02/2005

of the crystallization process of polymers. The detailed procedure for the construction of 2D IR correlation spectra, as well as their interpretation, may be found elsewhere.[13−15]

Recently, by applying the generalized 2D IR correlation analysis to the study of isothermal crystallization process of a polymer, we investigated successfully the structural changes taking place during the induction period of isotactic polystyrene (iPS) cold crystallization.[16] The structural evolution and crystallization dynamics of poly(L-lactide) (PLLA) during the isothermal cold crystallization process were also explored by using 2D IR spectroscopy.[17] These studies demonstrate that 2D IR correlation spectroscopy can shed additional light on developing and perfecting the polymer crystallization theory that usually heavily relies on the small-angle X-ray scattering (SAXS), wide-angle X-ray diffraction (WAXD), and morphology data, such as atomic force microscopy (AFM) and transmission electron microscopy (TEM).

Poly(3-hydroxybutyrate) (PHB) is an optically active aliphatic polyester with a relative low glass transition temperature (around 5 °C) produced by bacterial fermentation.[18] Owing to its biosynthetic origin, it is free from any residual contaminating catalyst. Upon crystallization from the melt, the low level of heterogeneous nuclei present in the pure PHB often makes it a material of choice very often used for model studies of polymer crystallization and morphology.[19,20] It has been found that PHB crystallizes into a 2_1-helix with an approximately g^+g^+tt conformation, and the crystal structure of isolated PHB consists of an orthorhombic unit cell which contains two left-handed helical molecules in antiparallel orientation.[21] The thermal and melting behavior of PHB has been investigated by several research groups,[22−26] as it is related to many potential applications of this class of polymers. Particular attention has been paid to the interaction between the C=O and CH_3 groups of PHB. In our previous study,[25] the temperature-dependent wide-angle X-ray scattering (WAXS) study suggested that there are intermolecular interactions between the C=O and CH_3 groups in PHB, and the interactions decrease along the *a* axis of the crystal lattice of PHB with temperature. Subsequently, the existence and thermally induced changes of the C−H···O hydrogen bond between the C=O group and the CH_3 group were also verified by a temperature-dependent IR spectroscopy study of PHB.[26]

Another remarkable feature of PHB is that, although the isolated polymer is highly crystalline, the native PHB within cell granules are found only in the amorphous state.[27] Recently, Ezquerra et al.[28] also obtained stable amorphous PHB nanofilms at room temperature by a simple spin-coating method. Obviously, it is an important and interesting work to suggest the mechanism, which inhibits the crystallization process of PHB under these confined conditions. However, we notice that the crystallization mechanism, even for the bulk PHB, is still unclear, and relatively few reports focus on studying its crystallization process.[22,29]

In the present study, using conventional spectral analysis methods for IR spectra, such as difference spectra and second derivatives, together with 2D correlation analysis, the spectral changes and molecular dynamics of PHB during the melt-crystallization at 129 °C are investigated in detail. Our results show that a band at 1731 cm^{-1}, which may be related to the intermediate state, does exist in the melt-crystallization process of PHB, and the structural adjustments of various functionalities in a polymer chain are cooperative and sequential.

2. Experimental Section

2.1. Material and Sample Preparation Procedures. Bacterially synthesized PHB was obtained from the Procter and Gamble Co., Cincinnati, OH. It was dissolved in hot chloroform, reprecipitated in methanol as fine powder, and vacuum-dried at 60 °C. A PHB film for an IR measurement was cast on KBr windows from a 1% (w/v) PHB chloroform solution. After the majority of the solvent had evaporated, the film was placed under vacuum at room temperature for 48 h to completely remove the residual solvent. Special attention was paid to ensure that the film examined was sufficiently thin (typically thickness is about 10 μm) to be within the absorption range where the Beer−Lambert law is obeyed. That is, the absorbance intensities of the strongest C=O stretching bands of PHB were controlled under 1.0 absorbance unit.

2.2. FTIR Spectroscopy. For the IR study of the melt-crystallization process of PHB, the KBr windows with the sample was set on a homemade variable temperature cell, which was placed in the sample compartment of a Nicolet Magna 870 spectrometer equipped with a MCT detector. The sample was first heated at 10 °C/min up to 195 °C (about 25 °C above the melting point) for 1 min to melt the polymer and erase the thermal history. Then, it was cooled at 5 °C/min to 129 °C for isothermal melt-crystallization. During the cooling period, we monitored structural changes in PHB with real-time IR measurements. From the real-time IR spectra, we found that there was no crystallization occurring immediately after the sample was cooled to 129 °C and that the crystallization rate under this temperature was also suitable for our real-time IR measurement. From the IR spectra, it was also found that 6 h is needed for finishing the crystallization at 129 °C. IR spectra of the specimen were collected at a 2 cm^{-1} resolution with a 2 min interval during the annealing process. The spectra were obtained by coadding 16 scans.

2.3. 2D IR Correlation Analysis. Before performing the 2D correlation analysis, the IR spectra were preprocessed to minimize the effects of baseline instabilities and other nonselective effects. The wavenumber regions of interest were truncated first and subjected to a linear baseline correction, followed by offsetting to the zero absorbance value. Sixteen spectra with an equal time interval in a certain wavenumber range were selected for the 2D correlation analysis, which was carried out by using the software named "2D Pocha" composed by D. Adachi (Kwansei Gakuin University). The time-averaged 1D reference spectrum is shown at the side and top of the 2D correlation maps for reference. In the 2D correlation maps, areas without dots indicate positive correlation intensities, while those with dots indicate negative correlation intensities.

3. Results and Discussion

3.1. CH Stretching Region. The time-dependent spectral evolution in the C−H stretching region during the melt-crystallization process of PHB at 129 °C is shown in Figure 1a. It can be seen that many new spectral features appear with the PHB sample transforming from the amorphous state to the semicrystalline state. To make these spectral changes clearer, difference spectra shown in Figure 1b were calculated by the subtraction of the initial spectrum from the spectra shown in Figure 1a. Figure 1c shows the second derivatives of the spectra measured at the beginning (0 min) and the end (300 min). From the second derivative spectra (Figure 1c), it can be seen that three obvious bands (2986, 2937, and 2878 cm^{-1}) can be detected for the amorphous sample. These bands are assigned to CH_3 stretching modes, CH_2 stretching modes, and CH

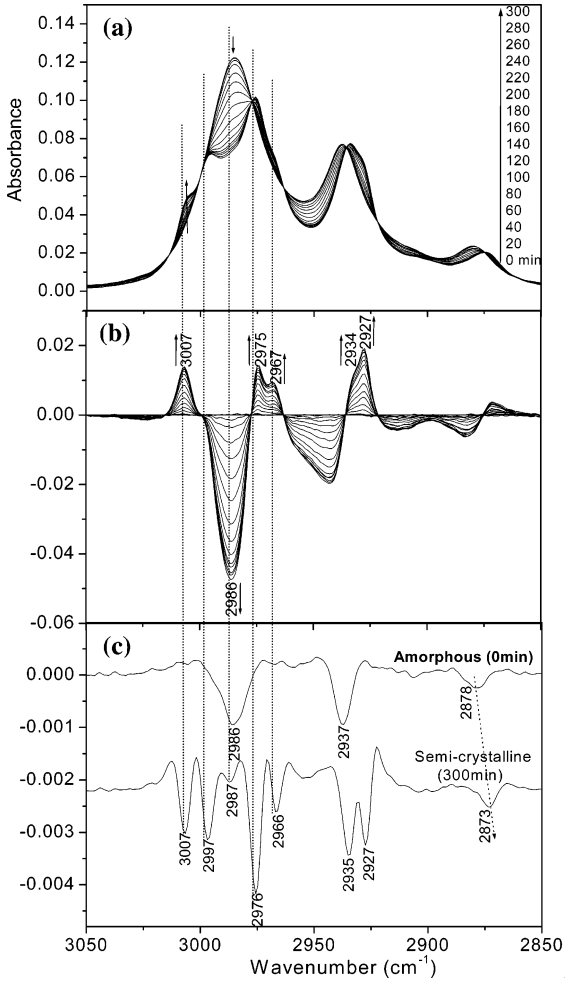

Figure 1. (a) Temporal changes in the IR spectrum in the range of 3050−2850 cm^{-1} during the melt-crystallization process of PHB at 129 °C. The spectra were arranged with a 20 min interval. (b) Difference spectra obtained by the subtraction of the initial spectrum from the spectra shown in (a). (c) Second derivatives of the spectra measured at 0 and 300 min.

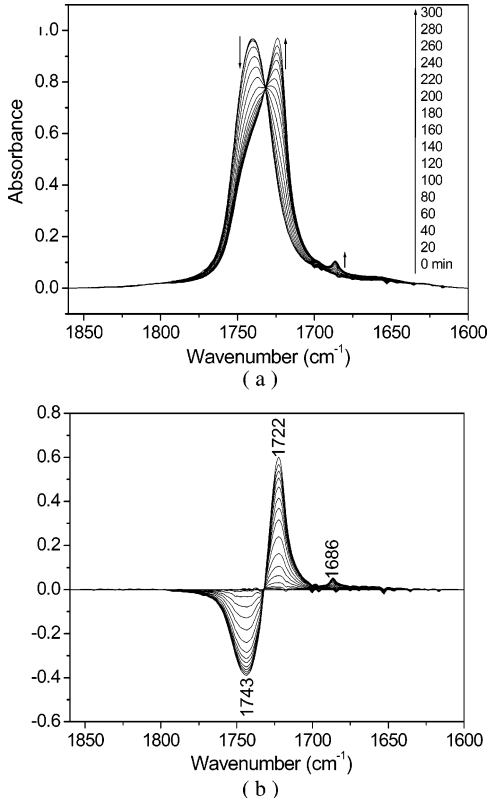

Figure 2. (a) Temporal changes of the IR spectrum in the range of 1860−1600 cm^{-1} during the melt-crystallization process of PHB at 129 °C. The spectra were arranged with a 20 min interval. (b) Difference spectra obtained by the subtraction of the initial spectrum from the spectra shown in (a).

stretching modes, respectively.[22,26,30] For the semicrystalline sample, the situation become complex, and there are eight bands (3007, 2997, 2987, 2976, 2966, 2935, 2927, and 2873 cm^{-1}) in the C−H stretching region. The difference spectra clearly demonstrate that the intensities of the bands at 3007, 2976, 2966, 2935, and 2927 cm^{-1} increase gradually with the development of the crystalline structure of PHB. Among these crystalline bands, the two pairs of bands, the bands at 2976 and 2966 cm^{-1} and those at 2935 and 2927 cm^{-1}, may result from the crystal field splitting. Usually, the crystal field splitting can be caused by the intermolecular interaction due to molecular packing in a crystal unit or the intramolecular interaction due to the formation of helix structure.[31,32] It has been found that PHB crystallizes into a left-handed 2_1-helix with the antiparallel alignment in a unit cell.[17] Thus, crystal field splitting should be responsible for the two new band pairs. An interesting observation is made that there is no significant change in the intensity of the band at 2997 cm^{-1} from the difference spectra (Figure 1b), although it can be clearly detected in the second derivative spectrum of semicrystalline sample. We assigned the band to a crystalline band before.[33,34] However, we reconsider this assignment after checking the second derivative spectrum (Figure 1c) of amorphous sample in detail. It is easy to find that the peak shape around 2986 cm^{-1} is not symmetric on the high-frequency side. Therefore, the band at 2997 cm^{-1} should already exist in the amorphous state and is not a crystalline sensitive band.

There are two other interesting spectral changes in the C−H stretching region during the melt-crystallization process of PHB at 129 °C. First, the CH stretching band shifts from 2878 to 2873 cm^{-1}. Such low-frequency shift should be correlated to the disordered to ordered conformational transition of PHB in the crystallization process. Second, a new band appears at 3007 cm^{-1} as a symmetric positive peak in the difference spectra (Figure 1b), and its intensity increases with the annealing time. Obviously, this band should be assigned to a crystalline band.[26] It has been well-known that CH_3 asymmetric stretching bands appear in the 2900−3000 cm^{-1} region. Thus, the appearance of the CH_3 asymmetric stretching band at 3007 cm^{-1} is rather unusual. Recently, several research groups[35−37] reported that the appearance of a CH_3 asymmetric stretching band above 3000 cm^{-1} indicates the existence of a C−H···O hydrogen bond. In our previous IR study on the thermal behavior of PHB, we demonstrated a peak shift for the band around 3007 cm^{-1}. On the basis of this observation together with the results of WAXD, we suggested that there is a CH_3···O=C intermolecular hydrogen bond in PHB crystals.[29] We will analyze this band again by 2D correlation analysis later.

3.2. C=O Stretching Region. Figure 2a shows spectral changes in the C=O stretching region during the melt-crystallization process of PHB at 129 °C. In the corresponding difference spectra (Figure 2b), the

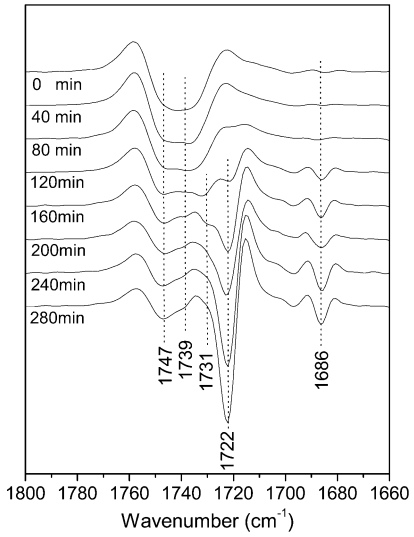

Figure 3. Second derivatives of the spectra measured during the isotherm crystallization process of PHB at 129 °C. The spectra were arranged with a 40 min interval from 0 to 280 min.

intensity of a positive peak at 1722 cm^{-1} increases gradually with time, while that of a negative peak at 1743 cm^{-1} decreases during the crystallization process. It seems rational to assign the 1722 cm^{-1} band to the ν(C=O) for the crystalline phase and the 1743 cm^{-1} band to the ν(C=O) for the amorphous phase.[25,26,34,38]

However, from the second derivatives (Figure 3) of the spectra shown in Figure 2a, four bands at 1747, 1739, 1731, and 1722 cm^{-1} can be detected in the 1780−1700 cm^{-1} region during the crystallization process. Among these bands, the 1747 and 1739 cm^{-1} bands already exist in the amorphous state. The quantum chemical calculations by Dybal et al.[39] indicate that the two C=O stretching bands arise from the different conformations of the main chain. Surprisingly, two crystalline bands appear in the crystallization process, although the 1731 cm^{-1} band cannot be detected evidently form the spectra obtained at the end of the crystallization process. In our previous study, the band at 1722 cm^{-1} was ascribed to the crystalline packing.[21] That is, it is correlated to the antiparallel alignment of the 2_1 helix chain in a unit cell. However, the assignment on the 1731 cm^{-1} band is not clear.[34,38] By using a curve fitting, Yoshie et al.[38] found three bands in the C=O stretching band region of semicrystalline PHB and assigned the bands at 1728 and 1722 cm^{-1} to the interfacial and crystalline phases, respectively. Usually, for the semicrystalline polymer, the amount of the interphase between the lamellar crystallites and amorphous layers should gradually increase with the crystallization time. Thus, it is rational to speculate that the intensity of the "interphase band" would also gradually increase during the crystallization process. However, the intensity of the band at 1731 cm^{-1} tends to decrease in the late period of the crystallization process as displayed in the second derivative spectra (Figure 3). Therefore, it may be more suitable to relate this band to "intermediate state" rather than "interphase" for explaining the spectral changes in the ν(C=O) region during the melt-crystallization process of PHB.

Padermshoke et al.[33] also observed the 1731 cm^{-1} band on investigating the melting behavior of PHB by 2D IR spectroscopy and assigned the weak band at 1731 cm^{-1} to the crystalline part with a less ordered

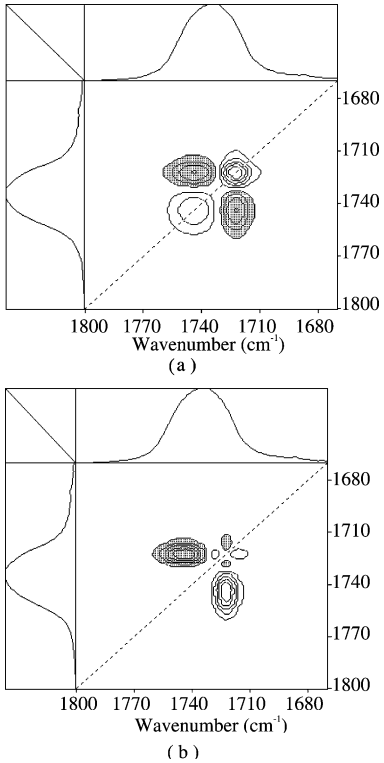

Figure 4. Synchronous (a) and asynchronous (b) 2D IR correlation spectra of PHB, in the ν(C=O) region, calculated from the spectra obtained during the isotherm crystallization process at 129 °C.

structure. Although there is no accurate definition for the concept of "intermediate state" or "less ordered structure" in the literature, they both reflect that there is a different physical state between the amorphous and crystalline states for the semicrystalline polymer. The assignment of "intermediate state" supports Strobl's multistep crystallization model mentioned in the Introduction. That is, there is an intermediate state during the formation and growth process of PHB lamellar crystallites. If such conjecture is correct, there should be a sequential change for these amorphous and crystalline C=O bands. To check this point, 2D correlation spectroscopy is employed.

Parts a and b of Figure 4 show the synchronous $\Phi(\nu_1,\nu_2)$ and asynchronous $\Psi(\nu_1,\nu_2)$ 2D correlation spectra, respectively, in the region of 1800−1670 cm^{-1} generated from the time-dependent spectra obtained during the crystallization process at 129 °C. In the synchronous spectrum, two autopeaks developed around 1743 and 1722 cm^{-1} together with negative cross-peaks at (∼1743, 1722) cm^{-1} indicate the spectral variations of the amorphous and crystalline components of the PHB polymer. Three pairs of cross-peaks are observed at (∼1743, 1722), (1731, 1722), and (1722, 1715) cm^{-1} in the corresponding asynchronous spectrum. The unexpected band at 1715 cm^{-1} should correspond to "concave upward" lobe in the second derivative spectra (Figure 3). From the elongated shape of the cross-peak around (∼1743, 1722) cm^{-1} and the bands analysis above, it is rational to conclude that the cross-peak around 1743 cm^{-1} in the 2D spectra represents the changes in the two different amorphous conformation bands of the C=O group at 1747 and 1739 cm^{-1}.

The asynchronous spectrum represents sequential or successive changes of spectral intensities measured at υ_1 and υ_2. According to Noda's rule,[13] the sign of an

asynchronous cross-peak becomes positive if the intensity change at v_1 occurs predominantly before v_2 in the sequential order of t. It becomes negative, on the other hand, if the change occurs after v_2. This rule is, however, reversed if the corresponding synchronous intensity becomes negative, i.e., $\Phi(v_1,v_2) < 0$. Therefore, the information about the sequential changes of the four bands (1747, 1739, 1731, and 1722 cm^{-1}) in the ν(C=O) region can be derived from Figure 4. In the synchronous spectrum (Figure 4a), Φ (~1743, 1722) < 0, and in the corresponding asynchronous spectrum Ψ (~1743, 1722) < 0 and Ψ (1731, 1722) >0 (Figure 4b). These observations indicate that the sequential order of these bands is ~1743 cm^{-1} (1747 and 1739 cm^{-1}) > 1731 cm^{-1} > 1722 cm^{-1}, which is consistent with our conjecture above. That is, the existence of an intermediate state may be the reason why the decreases in the crystalline components do not proceed simultaneously with the increase in the amorphous component. There is no asynchronous cross-peak between the two amorphous ν(C=O) bands (1747 and 1739 cm^{-1}), which indicates that there is a cooperative conformational adjustment for the C=O group in the amorphous state. However, we should realize that there is no direct evidence to relate the 1731 cm^{-1} band to intermediate state yet. For making clear these sequence changes of ν(C=O) bands, further work is needed to explore the accurate assignment of these bands.

Another notable point in Figures 2 and 3 is that a very weak peak appears at 1686 cm^{-1}, and its intensity increases with the crystallization time. Obviously, it is a crystalline sensitive band; however, there is no assignment for this band in the literature. On the basis of its weak intensity and band position, we speculate that this band is related to the crystal defect which is caused by the interaction of an OH end group and a C=O group of PHB.

3.3. C−O−C Stretching and C−C Stretching Region. Figure 5a shows the temporal changes of the IR spectrum in the range of 1500−800 cm^{-1} during the melt-crystallization process of PHB at 129 °C. In this region, bands due to the CH_3 and CH bending vibrations and the C−O−C and C−C stretching vibrations are heavily overlapped, and band assignments are not straightforward. Relatively large changes occur in the C−O−C stretching region from 1300 to 1000 cm^{-1} and in the C−C backbone stretching region from 1000 to 800 cm^{-1}. Therefore, we mainly investigate the spectral changes in these two regions. To emphasize the spectral changes and to relate the intensity changes of these peaks to the crystallization kinetics, difference spectra were calculated by subtracting the initial (amorphous state) spectrum from the rest of spectra in Figure 5a and are displayed in Figure 5b. In the region of 1300−1000 cm^{-1}, a band at 1184 cm^{-1} is characteristic of the asymmetric stretching vibration of the C−O−C group, and its intensity decreases largely with the crystallization time. Bloembergen et al.[40] had estimated the degree of crystallinity of PHB by following the relative intensity of this band, which displays the largest difference in intensity in the 1500−800 cm^{-1} region between the crystalline and amorphous states and is better resolved than the other crystalline bands.

However, little study has been reported on the band assignments of the C−C stretching vibration region (1000−800 cm^{-1}). The spectral changes in this region are very interesting and pronounced as shown in its

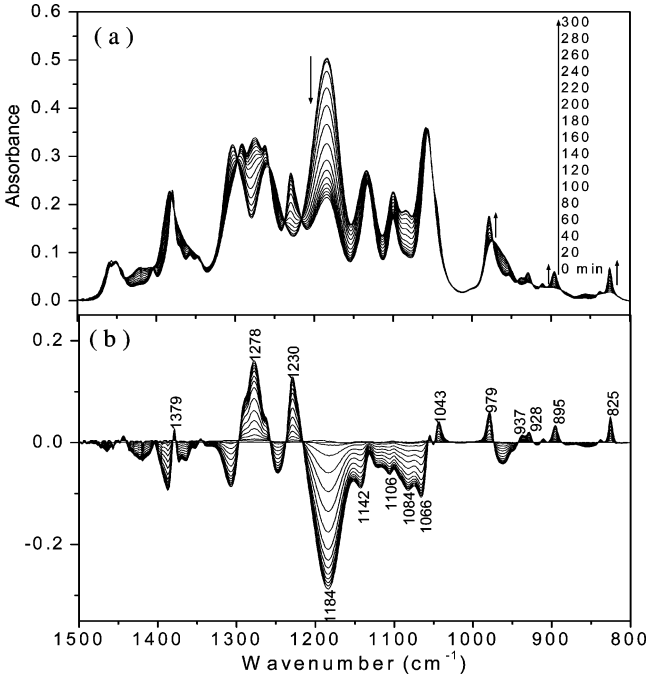

Figure 5. (a) Temporal changes of the IR spectrum in the range of 1500−800 cm^{-1} during the melt-crystallization process of PHB at 129 °C. The spectra were collected with a 20 min interval. (b) Difference spectra obtained by the subtraction of the initial spectrum from the spectra shown in (a).

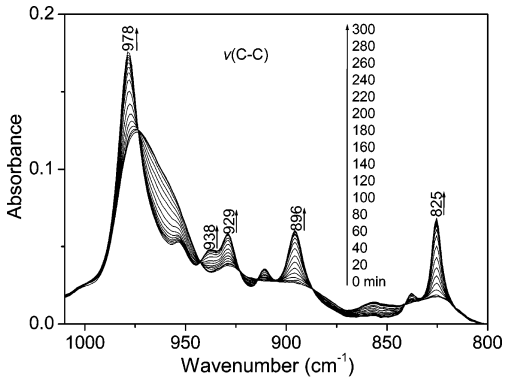

Figure 6. Enlarged spectral changes in the range of 1000−800 cm^{-1} during the melt-crystallization process of PHB at 129 °C.

enlarged spectra (Figure 6). Five crystalline bands at 978, 938, 929, 896, and 825 cm^{-1} can clearly be identified form both the enlarged spectra (Figure 6) and the difference spectra (Figure 5b). We notice that a part of the molecular structure in the repeat unit of PHB is the same as that of polypropylene (PP) and that bands due to the helical forms of sPP and iPP appear in the range of 1000−800 cm^{-1}.[41,42] Therefore, it is natural to propose that these crystalline bands of PHB appearing in the range of 1000−800 cm^{-1} are correlated to the formation of the 2_1 helix structure of PHB chain.

To investigate the crystallization kinetics, normalized peak heights of the crystalline sensitive bands of PHB at 1184 and 825 cm^{-1} calculated from the difference spectra (Figure 5b) are plotted in Figure 7a as a function of the crystallization time at 129 °C. It is interesting to note that there is an obvious lag between the change rates of these two bands. The 1184 cm^{-1} band shows the faster rate of change than the 825 cm^{-1} band. That is, the adjustment of C−O−C backbone is faster than that of C−C backbone. Usually, it has been believed that

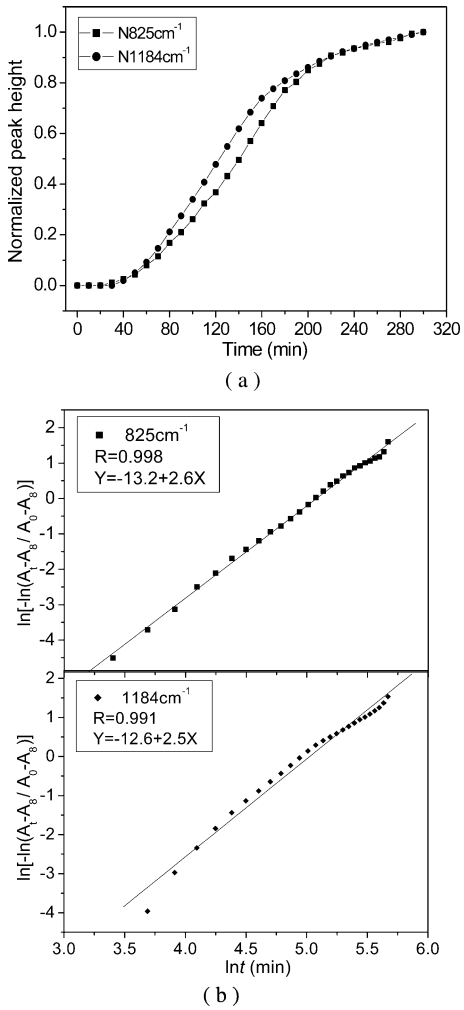

Figure 7. (a) Normalized peak heights of the crystalline sensitive bands at 1184 and 825 cm^{-1} of PHB as a function of crystallization time at 129 °C. (b) Avrami plot of the crystallization dynamics of PHB at 129 °C.

the structural changes of various functionalities within a polymer occur cooperatively during the crystallization process. However, in the case of melt-crystallization of PHB, the different rates of the structural changes are clearly demonstrated for the C−O−C and C−C backbones from Figure 7a. In our previous study on the cold crystallization of poly(L-lactide) (PLLA),[17] we also found that there is a sequential change for the methyl and ester groups. These observations indicate that, in some cases, the structural adjustments of various functionalities in a polymer chain are sequential and not cooperative.

When IR data in difference spectra are used, Avrami's equation[43] can be stated as follows:

$$\frac{A_t - A_\infty}{A_0 - A_\infty} = \exp(-kt^n) \tag{1}$$

where A_t is the peak intensity at the crystallization time t, A_∞ and A_0 are respectively the initial and final peak intensities during isothermal crystallization, k is the crystallization rate constant dependent on the nucleation and growth rates, t is the time of the crystallization, and n is Avrami exponent, which is related to the nature of nucleation and to the geometry of the growing crystals.[44] Equation 1 can also be expressed in the following form:

$$\ln\left[-\ln\left(\frac{A_t - A_\infty}{A_0 - A_\infty}\right)\right] = \ln k + n \ln t \tag{2}$$

Accordingly, the Avrami parameters n and k can be obtained from the slope and the intercept, respectively, by plotting the first term vs ln t. Figure 7b shows the Avrami plots of the crystallization dynamics of PHB at 129 °C obtained by using the data in Figure 7a. It is found that the linear relation of the Avrami plot is better represented by the data of the 825 cm^{-1} band than that of the Avrami plot by the data of the 1184 cm^{-1} band, although the Avrami exponents ($n \approx 2.6$ and 2.5, respectively) calculated from the two bands are almost the same. It should be noted that the use of Avrami analysis may not be strictly appropriate as the deviation from linearity is observed in Figure 7 Obviously, C−C backbone mode at 825 cm^{-1} is better than that of the C−O−C mode at 1184 cm^{-1} to reflect the crystallization dynamic of PHB by using Avrami analysis. This result also indicates that the crystallization dynamics of the C−O−C backbone is different from that of the C−C backbone of PHB. Evidence will be provided later about the sequential changes instead of the strictly cooperative and constant crystal growth rate.

3.4. 2D Correlation Analysis in Different Spectral Regions. From the analysis above, it is found that there is an intermediate state in the melt-crystallization process of PHB at 129 °C, and the structural adjustment of C−O−C and C−C backbones is not fully cooperative. To confirm these conclusions and to get a more precise picture on the molecular evolution during the melt-crystallization process of PHB, we further investigate 2D correlation spectra of PHB between different spectral regions.

Parts a and b of Figure 8 show the synchronous $\Phi(\nu_1,\nu_2)$ and asynchronous $\Psi(\nu_1,\nu_2)$ 2D correlation spectra obtained by correlating the 1300−1000 cm^{-1} region with the 1000−800 cm^{-1} region of PHB, calculated from the spectra obtained during the melt-crystallization process at 129 °C, respectively. Unexpectedly, in the 1300−1000 cm^{-1} region, only the band at 1184 cm^{-1} generates an asynchronous cross-peak with bands in the 1000−800 cm^{-1} region. The presence of the asynchronous cross-peaks reflects the difference in the mobility between the C−O−C backbone and C−C backbones. In the synchronous spectrum (Figure 8a), $\Phi(1184, 825) < 0$, and in the corresponding asynchronous spectrum $\Psi(1184, 825) < 0$, which verifies that the change of the C−O−C band at 1184 cm^{-1} occurs prior to that in the C−C band at 825 cm^{-1} in PHB.

We have indicated that the spectral changes in the C=O stretching region are very interesting during the melt-crystallization process of PHB. Therefore, more information is expect to be obtained about the crystallization process of PHB by correlating the C=O stretching band region with the 1300−1000 and 1000−800 cm^{-1} regions of PHB. The synchronous and asynchronous 2D correlation spectra correlating the C=O band stretching region with the 1000−800 cm^{-1} region of PHB are displayed in parts a and b of Figure 9, respectively. From the observations that $\Phi(\sim1743, 825) < 0$ and $\Phi(1722, 825) > 0$ in the synchronous spectrum (Figure 9a) and $\Psi(\sim1743, 825) < 0$ and $\Psi(1722, 825) < 0$ in the corresponding asynchronous spectrum (Figure 9b), the sequential order of these bands is derived as follows: ~1743 cm^{-1} > 825 cm^{-1} > 1722 cm^{-1}.

Similarly, parts a and d of Figure 9 illustrate the synchronous and asynchronous 2D correlation spectra

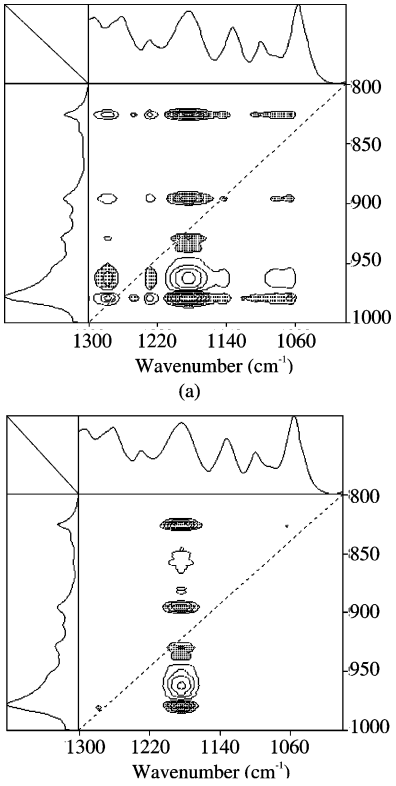

Figure 8. Synchronous (a) and asynchronous (b) 2D IR correlation spectra correlating the 1300−1000 cm^{-1} region with the 1000−800 cm^{-1} region of PHB, calculated from the spectra obtained during the melt-crystallization process at 129 °C.

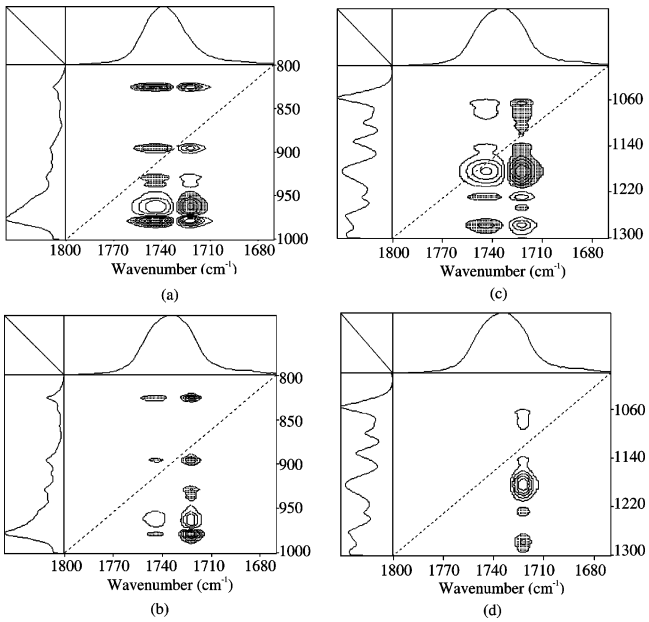

Figure 9. Synchronous (a, c) and asynchronous (b, d) 2D IR correlation spectra correlating the 1800−1670 cm^{-1} region with the 1000−800 and 1300−1000 cm^{-1} regions of PHB, respectively, calculated from the spectra obtained during the melt-crystallization process at 129 °C.

correlating the C=O stretching region with the 1300−1000 cm^{-1} region, respectively. Observations of $\Phi(\sim 1722, 1184) < 0$ in the synchronous spectrum (Figure 9c) and $\Psi(1722, 1184) < 0$ in the corresponding asynchronous spectrum (Figure 9d) indicate that the change of the C−O−C band at 1184 cm^{-1} occurs prior

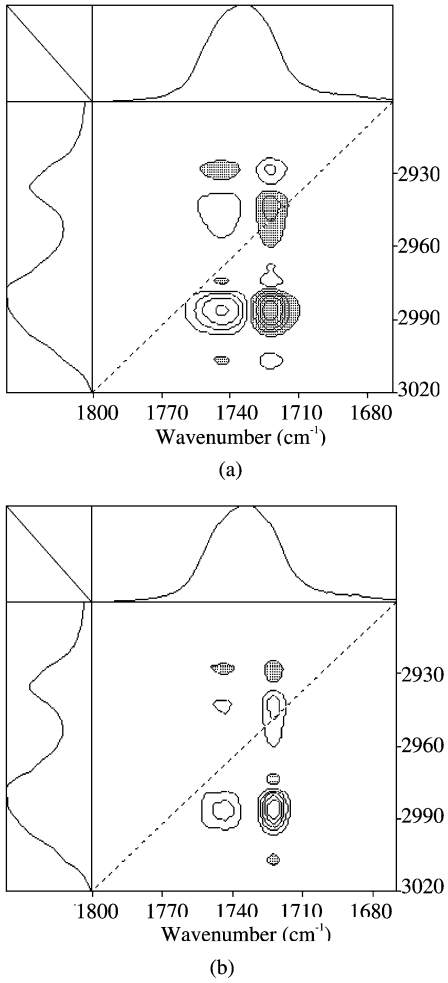

Figure 10. Synchronous (a) and asynchronous (b) 2D IR correlation spectra correlating the 1800−1670 cm^{-1} region with the 3020−2900 cm^{-1} region of PHB, respectively, calculated from the spectra obtained during the melt-crystallization process at 129 °C.

to that of the C=O band at 1722 cm^{-1}. Moreover, no asynchronous cross-peak is shared between the C=O band at 1743 cm^{-1} and the bands in the C−O−C stretching vibration region (Figure 9d), indicating that there is a cooperative change between them.

In the above analysis, the band centered around 1743 cm^{-1} in the 2D IR spectra has been assigned to the C=O stretching vibration band for the amorphous state which, in fact, consists of the two amorphous ν(C=O) bands at 1747 and 1739 cm^{-1}, and the 1722 cm^{-1} band reflects the antiparallel alignment of the 2_1 helix chain of PHB in a unit cell. Furthermore, the 825 cm^{-1} band is ascribed to the 2_1 helix band of PHB. Therefore, the physical origin of the sequential order of these bands is that the melt-crystallization of PHB is accompanied by a conformational rearrangement of the various functionalities of PHB. The C=O group and the C−O−C group rearrange their conformations cooperatively first; that is, the ester groups adjust their conformation as a whole, which leads to the conformation adjustment of C−C backbone for forming the 2_1 helical chain geometries. At last, the 2_1 helix chains pack into the crystal unit cell.

Figure 10a,b shows the synchronous and asynchronous 2D correlation spectra correlating the C=O stretching band region with the CH stretching band region of PHB. It is noted that there is a cross-peak between the

3007 cm^{-1} band due to the asymmetric CH_3 stretching mode and the 1722 cm^{-1} band arising from the antiparallel alignment of the 2_1 helix chain of PHB in a unit cell in the asynchronous spectrum (Figure 10b). The presence of this asynchronous cross-peak suggests that their changes are out of phase with each other. Moreover, the correlation intensities $\Phi(1722, 3007) > 0$ and $\Psi(1722, 3007) < 0$ indicate that the change of the 3007 cm^{-1} band occurs prior to that of the 1722 cm^{-1} band. This result suggests that, before the closed packing of the 2_1 helix chains of PHB, the $CH_3\cdots O{=}C$ hydrogen bond already appears.

4. Conclusion

The IR spectral changes and band assignments during the melt crystallization of PHB have been investigated in detail by conventional spectral analysis methods as well as 2D correlation analysis. In the C=O stretching band region, five bands (1747, 1739, 1731, 1722, and 1686 cm^{-1}) have been clearly detected. Among these bands, changes in the two amorphous bands at 1747 and 1739 cm^{-1} are cooperative, whereas the change in the 1731 cm^{-1} band, which had been assigned to the intermediate phase by other researchers,[38] and that in the 1722 cm^{-1} band due to the crystal packing are out of phase with each other. The existence of the 1731 cm^{-1} band is suggested by the second derivative and 2D correlation analysis, but the direct evidence relating the 1731 cm^{-1} band to the intermediate state or intermediate phase is still lacking. Further studies by using other techniques are probably needed to clarify the origin of the 1731 cm^{-1} band. It has been commonly believed that the structural changes of various functionalities within a polymer occur cooperatively during the crystallization process. However, at least in the melt-crystallization of PHB, a different rate of changes is observed for the C−O−C and C−C backbones according to the peak height changes in the difference spectra and the presence of cross-peaks in the asynchronous 2D IR spectra. Moreover, in our previous study on the cold crystallization of PLLA,[17] the sequential change for the methyl and ester groups was also monitored. Our observations indicate that not only the "cooperativity" but also the "sequential change" is one of the important characteristics for the structural adjustment of polymer chains in the crystallization process of certain polymers. These sequential changes in IR bands are interpreted as follows: In the crystallization process of PHB, the ester groups, as localized and flexible moieties, instantly adjust their conformation. Longer regular 2_1 helix chain sequences then develop through annealing. Finally, these regular 2_1 helix sequences pack into the crystal unit cell, which takes the longest annealing time.

Acknowledgment. Jianming Zhang thanks the Japan Society for the Promotion of Science (JSPS) for financial support.

References and Notes

(1) Strobl, G. R. *The Physics of Polymers*; Springer-Verlag: Berlin, 1997.
(2) Lauritzen, J. H.; Hoffmann, J. D. *Natl. Bur. Stand.* **1960**, *64A*, 73−102.
(3) Sadler, D. M. *Polymer* **1983**, *24*, 1401−1409.
(4) Lotz, B. *Eur. Phys. J. E* **2000**, *3*, 185−194.
(5) Cheng, S. Z. D.; Li, C. Y.; Zhu, L. *Eur. Phys. J. E* **2000**, *3*, 195−197.
(6) Strobl, G. *Eur. Phys. J. E* **2000**, *3*, 165−183.
(7) Chalmers, J. M.; Hannah, R. W.; Mayo, D. W. Spectra-Structure Correlations: Polymer Spectra. In *Handbook of Vibrational Spectroscopy*; Chalmers, J. M., Griffiths, P. R., Eds.; John Wiley & Sons: Chichester: UK, 2002; Vol. 4, pp 1893−1918.
(8) Koenig, J. L. *Spectroscopy of Polymers*; American Chemical Society: Washington, DC, 1992.
(9) Mallapragada, S. K.; Narasimhan, B. Infrared Spectroscopy in Analysis of Polymer Crystallinity. In *Encyclopedia of Analytical Chemistry*; Meyers, R. A., Ed.; John Wiley & Sons: Chichester, UK, 2000; pp 7644−7658.
(10) Heintz, A. M.; McKiernan, R. L.; Gido, S. P.; Penelle, J.; Hsu, S. L. *Macromolecules* **2002**, *35*, 3117−3125.
(11) Zhu, X. Y.; Yan, D. Y.; Fang, Y. P. *J. Phys. Chem. B* **2001**, *105*, 12461−12463.
(12) Duan, Y. X.; Zhang, J. M.; Shen, D. Y.; Yan, S. K. *Macromolecules* **2003**, *36*, 4847−4879.
(13) Noda, I. *Appl. Spectrosc.* **1993**, *47*, 1329−1336.
(14) Noda, I.; Ozaki, Y. *Two-Dimensional Correlation Spectroscopy*; John Wiley & Sons: Chichester, UK, 2004.
(15) Noda, I.; Dowrey, A. E.; Marcott, C.; Story, G. M.; Ozaki, Y. *Appl. Spectrosc.* **2000**, *54*, 236A.
(16) Zhang, J. M.; Duan, Y. X.; Shen, D. Y.; Yan, S. K.; Noda, I.; Ozaki, Y. *Macromolecules* **2004**, *37*, 3292−3298.
(17) Zhang, J. M.; Tsuji, H.; Noda, I.; Ozaki, Y. *Macromolecules* **2004**, *37*, 6433−6439.
(18) Lageveen, R. G.; Huisman, G. W.; Preusting, H.; Ketelaar, P.; Eggink, G.; Witholt, B. *Appl. Environ. Mocrobiol.* **1988**, *54*, 2924−1931.
(19) Barham, P. J.; Keller, A.; Otun, E. L.; Hormes, P. A. *J. Mater. Sci.* **1984**, *19*, 2781−2794.
(20) Barham, P. J. *J. Mater. Sci.* **1984**, *19*, 3826−3824.
(21) Yokouchi, M.; Chatani, Y.; Tadokoro, H.; Teranishi, K.; Tani, H. *Polymer* **1973**, *14*, 267−272.
(22) Xu, J.; Guo, B.; Yang, R.; Wu, Q.; Chen, G.; Zhang, Z. *Polymer* **2002**, *43*, 6893−6899.
(23) Wu, Q.; Tain, G.; Sun, S.; Noda, I.; Chen, G.-Q. *J. Appl. Polym. Sci.* **2001**, *82*, 934−940.
(24) Abe, H.; Doi, Y.; Aoki, H.; Akehata, T. *Macromolecules* **1998**, *31*, 1791−1797.
(25) Sato, H.; Nakamura, M.; Padermshoke, A.; Yamaguchi, H.; Terauchi, H.; Ekgasit, S.; Noda, I.; Ozaki, Y. *Macromolecules* **2004**, *37*, 3763−3769.
(26) Sato, H.; Murakami, R.; Padermshoke, A.; Hirose, F.; Senda, K.; Noda, I.; Ozaki, Y. *Macromolecules* **2004**, *37*, 7203−7213.
(27) Calvert, P. *Nature (London)* **1992**, *360*, 535.
(28) Capitan, M. J.; Rueda, D. R.; Ezquerra, T. A. *Macromolecules* **2004**, *37*, 5653−5659.
(29) Padermshoke, A.; Katsumoto, Y.; Sato, H.; Ekgasit, S.; Noda, I.; Ozaki, Y. *Polymer* **2004**, *45*, 7159−7165.
(30) Lambeek, G.; Vorenkamp, E. J.; Schouten, A. J. *Macromolecules* **1995**, *28*, 2023−2032.
(31) Nikimin, V. N.; Volchek, B. Z. *Russ. Chem. Rev.* **1968**, *37*, 225−239.
(32) Lagaron, J. M. *Macromol. Symp.* **2002**, *184*, 19−36.
(33) Padermshoke, A.; Katsumoto, Y.; Sato, H.; Ekgasit, S.; Noda, I.; Ozaki, Y. *Spectrochim. Acta, Part A* **2005**, *61*, 541−550.
(34) Padermshoke, A.; Sato, H.; Katsumoto, Y.; Ekgasit, S.; Noda, I.; Ozaki, Y. *Vib. Spectrosc.* **2004**, *36*, 241−249.
(35) Matsuura, H.; Yoshida, H.; Hieda, M.; Yamanaka, S.; Harada, T.; Shin-ya, K.; Ohno, K. *J. Am. Chem. Soc.* **2003**, *125*, 13910−13911.
(36) Harada, T.; Yoshida, H.; Ohno, K.; Matsuura, H. *Chem. Phys. Lett.* **2002**, *362*, 453−460.
(37) Boldeskul, I. E.; Tsymbal, I. F.; Ryltsev, E. V.; Latajka, Z.; Barnes, A. J. *J. Mol. Struct.* **1997**, *436/437*, 167−171.
(38) Yoshie, N.; Oike, Y.; Kasuya, K.; Doi, Y.; Inoue, Y. *Biomacromolecules* **2002**, *3*, 1320−1326.
(39) Dybal, J.; Sato, H.; Ozak, Y., to be published.
(40) Bloembergen, S.; Holden, D. A.; Hamer, G. K.; Bluhm, T. L. Marchessault, R. H. *Macromolecules* **1986**, *19*, 2865−2871.
(41) Natta, G.; Pasquon, I.; Corradini, P.; Peraldo, M.; Pegoraro, M.; Zambelli, A. *Rend. Accad. Naz. Lincei* **1960**, *28*, 539−546.
(42) Kobayashi, M.; Akita, K.; Tadokoro, H. *Makromol. Chem.* **1968**, *118*, 324−331.
(43) Avrami, M. *J. Chem. Phys.* **1939**, *7*, 1103−1112.
(44) Qin, Z. B.; Mo Z. S.; Zhang, H. F.; Sheng, S. R.; Song, C. S. *J. Polym. Sci., Part B: Polym. Phys.* **2000**, *38*, 1992−1997.

MA0501343